FLYWHEEL: JURNAL TEKNIK MESIN UNTIRTA

Homepagejurnal: http://jurnal.untirta.ac.id/index.php/jwl

Fitness For Service Assessment of Bulged Sewage Tank

Kasda[1*], Hari Din Nugraha[2], Rachman Setiawan [3]

[1]*Dept Mechanical Engineering. Universitas Subang, Subang 41285, Indonesia.*
[2]*Dept Mechanical Engineering. Universitas Subang, Subang 41285, Indonesia.*
[3]*Faculty of Mechanical and Aerospace Engineering. Institut Teknologi Bandung,, Bandung 40116, Indonesia*

*kasdakasdoels@gmail.com

ARTICLE INFO

Received 23/9/2020
Revision 12/11/2020
accepted 17/11/2020
Available online 23/11/2020

ABSTRACT

Based on the visual inspection and measurement, bulging was found on the Sewage Tank. There are cracks found in some areas of the welded joint on the tank wall. A suitable recommendation needs to be found for the equipment to be operated safely and reliably. The finite element simulation aims to estimate the tank's loading before the damage and provide a recommendation for repair, replacement, or other suitable options. Several ways have been carried out To estimate the cause of bulging. The sewage tank is modeled using a finite-element based software, under a normal up to the maximum allowable loading condition, using a linear-static analysis. Based on finite element simulation, under normal loading of 0.15 bar with 6 mm thickness, the tank is considered safe with a safety factor is 2.87, compared with a minimum specified Yield Strength of the material of 267 MPa. Whereas, under the high loading of 0.4 bar, the safety factor drops to 1.50. Due to the estimated loading case that caused the permanent deformation, some of the tank walls experience tensile residual stress. This condition is considered unsafe. Therefore, removal of the residual stress is required.

Keywords: *sewage tank, bulging, safety factor*

1. INTRODUCTION

A sewage tank is an equipment to decompose raw sewage before dispose of into the sea. Aerobic bacteria in the tank will decompose raw sewage. Therefore a continuous supply of fresh air (aeration) is significant; otherwise, an-aerobic bacteria will survive and produce toxic gases hazardous to health. An aeration tank was the main source of methane emission from all the units. Almost all the methane was emitted from the aeration tank [1]. The internal sewage tank consists of four main chambers; primary chamber, aeration chamber, settling tank, and chlorination & collection chamber [2] (Figure 1).

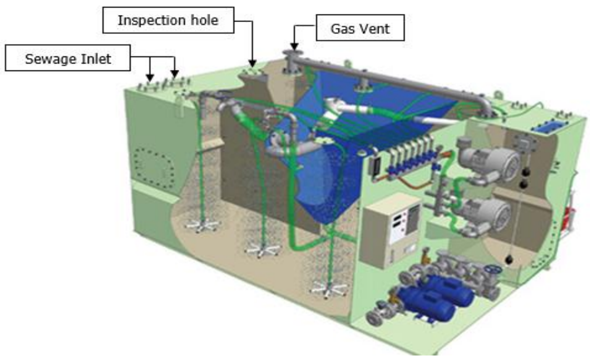

Figure 1. Typical construction of the sewage tank internal

The airflow pressure shall be controlled between 0.30-0.40 bar to allow a right mix between sewage and air (aerobic bacteria) and produce optimum decomposition. From the instruction manual, the process leading to a conclusion of normal mechanical loading can be found, among which a normal static pressure of 0.15 to 0.5 bar.

shows the plate thickness measurement data, with an illustration of the measurement location, as in Figure 2.

Table 1. Measurement result of Sewage Tank wall thickness [1].

	Measurement Point			
No	Front side	Right Side	Rear Side	Left Side
1	5,99	5,56	5,38	5,57
2	6,00	5,65	5,81	5,60
3	5,66	5,63	5,35	5,62
4	5,96	5,58	5,87	5,58
5	5,88	5,62	5,49	5,65
6	5,71	5,64	5,73	5,62
7	5,60	5,73	5,40	5,93
8	5,67	5,58	5,45	5,66
9	5,65	5,61	5,99	5,60
10		6,08	5,87	5,57
11		5,54	5,77	5,64
12		5,59	5,66	5,58
13		5,63		5,77
14		5,61		5,65
max.	6,00	6,08	5,99	5,93
min.	5,60	5,54	5,35	5,57
avg.	5,79	5,65	5,65	5,65

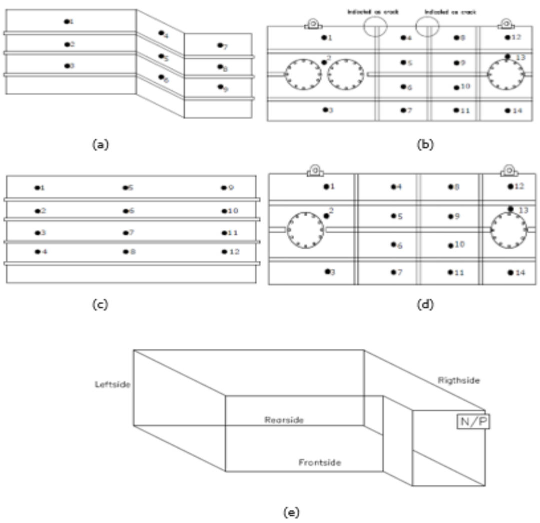

Figure 2. Information on locations of measurement points: a) Frontside, b) Rightside, c) Rearside, d) Leftside, e) Tank [3]

The tank plate material is SS400 structural steel, with typical mechanical properties (**Error! Reference source not found.**) [4]. From the instruction manual, the process leading to a conclusion of normal mechanical loading can be found, among which a normal static pressure of 0.15 to 0.5 bar.

Tabel 2. Mechanical properties of JIS 3101 SS 1/400

No	Property	Value
1	Tensile Strength, MPa	400-510
2	Yield Strength, min, MPa	267
3	Modulus elatisitas , GPa	190 - 210
4	Poisson ratio	0.3
5	Elongation (min.), %	17

After the inspection report, the damage was detected, consisting of permanent deformation on the overall tank, and several cracks on the stiffener. The data shows that the measured thickness values range from 5.35 to 6.08 mm, with an average of 5.67 mm. The nominal plate thickness upon installation is 6 mm.

The measurement of the permanent deformation, on the other hand, is illustrated in Figure 3. According to the measurement data, the maximum deformation is 47 mm, on the tank's left side[5]. The inspection did not include a visual examination of the tank internals.

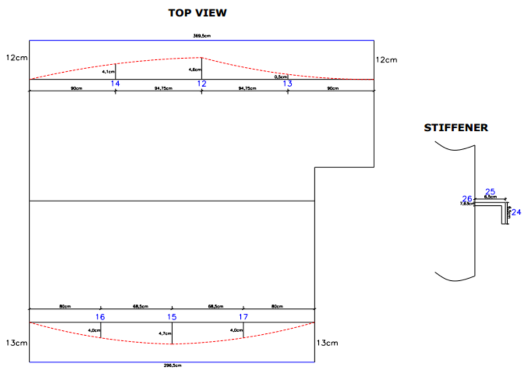

Figure 3. Illustration of permanent deformation on both sides of the sewage tank (Source: UT Inspection Report)

Residual stresses play significant roles in engineering structures, with highly beneficial effects when designed well and catastrophic effects when ignored [6]. Residual stresses can have a significant influence on the fatigue lives of structural engineering components [7]. Integral structures fabricated using welding present residual stresses, affecting their behavior, particularly fatigue crack propagation [8]. Based on the visual inspection and measurement, Bulging was found on the Sewage Tank. There are cracks found in some welded joint areas between the shell and external stiffener (Figure 4). Although not critical the long term effects of damage need to be assessed, and suitable recommendation needs to be found for the equipment to be operated safely and reliably.

Figure 4. Bulging on Sewage Tank

Finite Element Analysis (FEA) is a vital engineering tool used to approximate and verify how a component will react under various external and internal loading conditions [9]. A three-dimensional (3D) finite element analysis was performed to evaluate how the elastic properties of the fabrication material of dental implants influence peri-implant bone load transfer in terms of the magnitude and distribution of stress and deformation[10].

The finite element simulation aims to estimate the tank's loading before the damage and provide a recommendation for repair, replacement, or other suitable options. Finite Element Analysis (FEA) is the most appropriate technique in strength calculations of the structures working under known load and boundary conditions[11]. Stress analysis of a Bicycle frame is carried out using ANSYS Workbench 14.5 using various boundary conditions and compared with theoretical results [12]. Finite element analysis (FEA) is performed to achieve the variation of stress at critical areas of the crankshaft using the ANSYS software and apply the boundary conditions [13].

The sewage tank geometry is modeled using Autodesk Inventor 12 as a surface shell to allow the variation of the thickness more conveniently. Autodesk Inventor is a program specifically designed for engineering purposes such as product design, machine design, mold design, construction design, or other engineering purposes[14]. The finite element model is solved using ANSYS (Version 5.2, ANSYS Inc.) to obtain the Von Mises stress distributions[15].

The model is exported to Ansys workbench for finite element simulation. Ansys was used to build a computational model. build a partial model's likely geometrical model, material model, finite element model, and loading model is essential to obtain a correct and practical solution[16]

First, linear static analysis is carried out to model a normal working condition to the highest allowable average load. Another simulation strategy is also carried out, using elastic-plastic for comparison[17]. This loading case is simulated as a benchmark against the damaged condition. In the second phase, the simulation is carried out to estimate what kind of loading the tank has experienced that has plastic deformation as measured. The simulation is carried out for several trial cases iteratively.

2. METHOD

To estimate the cause of the sewage tank bulging, the following procedures have been carried out. Based on available information on the geometry, the sewage tank is modeled using a geometric modeling software as shell element [18]. Figure 5 and Figure 6. At a baselline, the sewage tank is modeled using a finite-element based software, under a normal up to the maximum allowable loading condition, using a linear-static analysis.

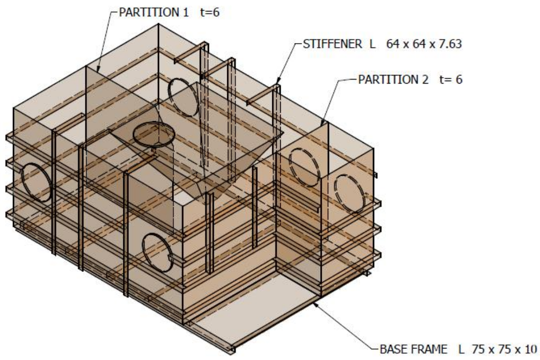

Figure 5. Surface shell model of the sewage tank (Showing it's internal)

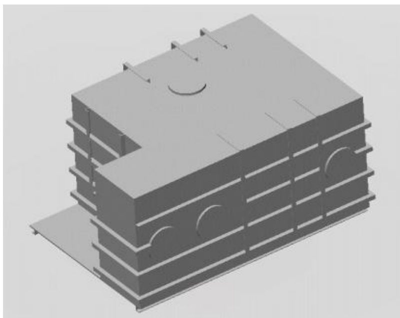

Figure 6. Surface shell model of the sewage tank (rendered model)

The influence of increasing strain rate on the mechanical behavior and deformation substructures in metals and alloys that deform predominately by slip is very similar to that seen following quasi-static deformation at increasingly lower temperatures [19]. The tank's permanent deformation is suspected to be caused by an abnormal loading condition due to either wall thinning or pressure accumulation, or both. Therefore, for the plastic deformation simulation, the material is modeled as an elastic-plastic model based on limited information and assumptions.

The condition that might have caused the damage is estimated through trials of several of potential load cases, until the permanent deformation from the simulation result match with that of measurement. With the possible cause of damage is estimated, the stress level, residual stress and critical locations can be estimated and recommendation based on these information is sought after.

Based on the information obtained from the Instruction Manual, the plate is made of SS 400 material. Typical material properties of JIS 3101 SS41/400 in **Error! Reference source not found.** has been used. For the analysis, two material modelling strategies have been used:

1. Linear-elastic model, to simulate normal working condition
2. Elastic-plastic model, to simulate the damaged condition, where plasticity is expected to have occurred.

For the first model, the finite element model uses only the Modulus of Elasticity of 210 GPa, and Poisson's ratio of 0.3. The second model uses a more complex material model, not only the above two elastic properties, but also plasticity data. Since no actual test data is available, the plasticity is assumed based on the information of Yield Strength of 267 MPa, Tensile Strength 400 MPa, and elongation of 17%, Figure 8 show the engineering data input in the finite element software for elastic and elastic-plastic model, respectively. Figure 9 shows the finite element model of the sewage tank after a meshing process [20].

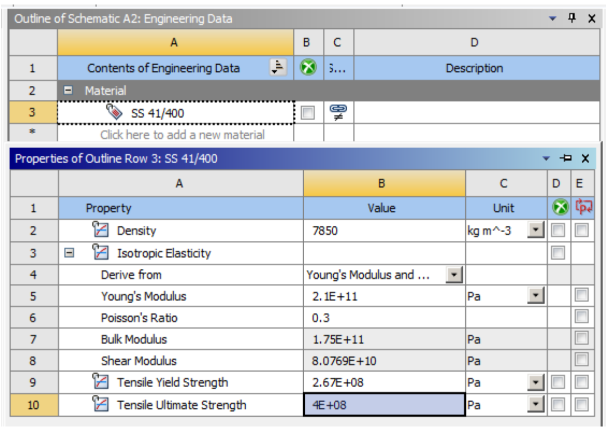
Outline of Schematic A2: Engineering Data

	A	B	C	D
1	Contents of Engineering Data		...	Description
2	Material			
3	SS 41/400			
*	Click here to add a new material			

Properties of Outline Row 3: SS 41/400

	A	B	C	D	E
1	Property	Value	Unit		
2	Density	7850	kg m^-3		
3	Isotropic Elasticity				
4	Derive from	Young's Modulus and ...			
5	Young's Modulus	2.1E+11	Pa		
6	Poisson's Ratio	0.3			
7	Bulk Modulus	1.75E+11	Pa		
8	Shear Modulus	8.0769E+10	Pa		
9	Tensile Yield Strength	2.67E+08	Pa		
10	Tensile Ultimate Strength	4E+08	Pa		

Figure 7. Engineering data set-up for linear elastic material model

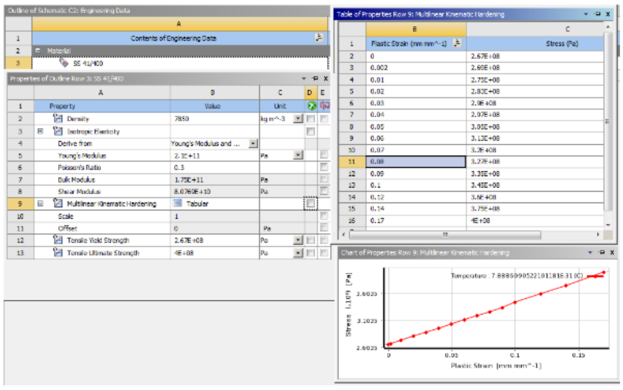

Figure 8. Engineering data set-up for elastic-plastic material model

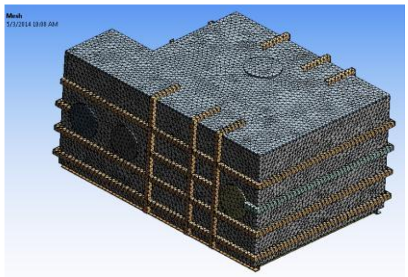

Figure 9. Meshing model of the sewage tank

3. RESULT AND DISCUSSION

The von Mises stress is often used as the metric for evaluating design margins, particularly for structures made of ductile materials [21]. Finite element analysis (FEA) and tests based on the Von Mises criterion have been applied in order to evaluate the stress distribution over two different prosthodontics retention systems [22]. The finite element model (FEM) of the residual stresses and strains that are formed after an elastoplastic hemispherical contact is unloaded. The material is modeled as elastic perfectly plastic and follows the von Mises yield criterion [23].

Table 2. Load cases under finite element simulation

Finite Element Model	Loading Case		
	1	2	3
Hydrostatic pressure load	√	√	√
Own-weight load	√	√	√
Static pressure load	0.4 and 0.15 bar	0.5 bar	(trials)
Wall thickness	6 mm	6 mm	(trials)
Material model	Linear Elastic	Linear-Elastic, and Elastic-Plastic	Elastic-Plastic

The finite element analysis result is presented in three basic load cases, as in Table 2. The result of each case shows equivalent stress in terms of von Mises stress distribution, and whichever necessary, including principal stress in order to determine the type of stress occurred, i.e. tensile or compressive stress. Apart from the stress, the deformation is also monitored, especially in the case of damaged condition, illustrating the plastic deformation.

3.1 Normal Loading Condition

This first loading case in Table 3, represents a normal working loading condition, with a static pressure of 0.15 bar (Load Case 1.1) and 0.4 bar (Load Case 1.2), among other loadings. With a linear elastic material model, the highest equivalent (von Mises) stress is estimated to be 92.95 MPa and 177.68 MPa, for Load Case 1.1 and 1.2, respectively. It occurs on the stiffener of the rightside of the tank.

Table 3 Load case combinations to simulate damage condition

Case No.	Static pressure (bar)	Thickness (mm)
3.01	0,5	5,80
3.02	1,0	5,35
3.03	1,5	5,67
3.04	2,0	6,00
3.05	2,1	5,35
3.06	2,2	5,35
3.07	2,3	5,67
3.08	2,4	6,00
3.09	2,5	6,00

By comparing with the material Yield Strength of 267 MPa, the normal working conditioin is the lowest safety factor for 2.87. The highest deformation is estimated to be 2.77 and 5.53 mm, for Load Case 1.1 and 1.2, respectively. Since, no plasticity occurs on the entire structure, no residual stress has been found and the tank is still within the elastic region.

The stress and deformation distribution for Load Case 1.1 can be seen in Figure 10 and Figure 11, whilst Figure 12 and Figure 13 for Load Case 1.2. The stress distribution for the linear-elastic and elastic-plastic model can be seen in Figure 14 and Figure 15 respectively. If the stress lies below the yield limit, the deformation is recoverable upon unloading. This behavior is called an elastic response [24]. One can compare that for both models, there is no significant difference in the stress result between these two material models. The maximum von Mises stress values are approximately 211 MPa, occurring at the same location, i.e. at the flange of the stiffener on the tank's left side wall, the same location on the average working loading condition. Again no plastic deformation occurs under this load case, with the safety factor approximately 1.26, drops from 2.87 under average working load.

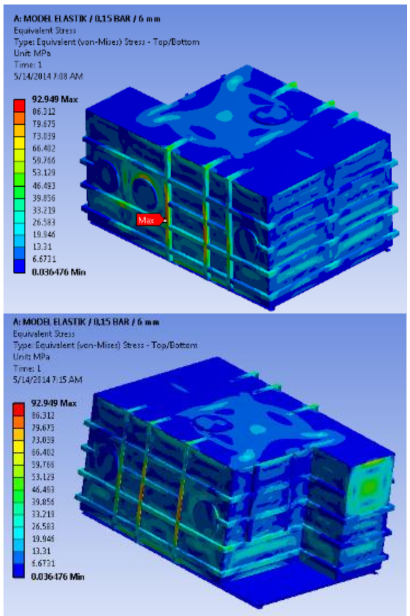

Figure 10. Von Mises stress distribution for normal working loading condition (Load Case 1.1)

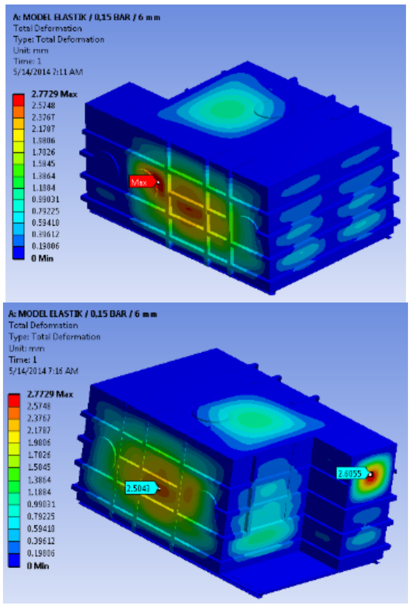

Figure 11. Deformation distribution for normal working loading condition (Load Case 1.1)

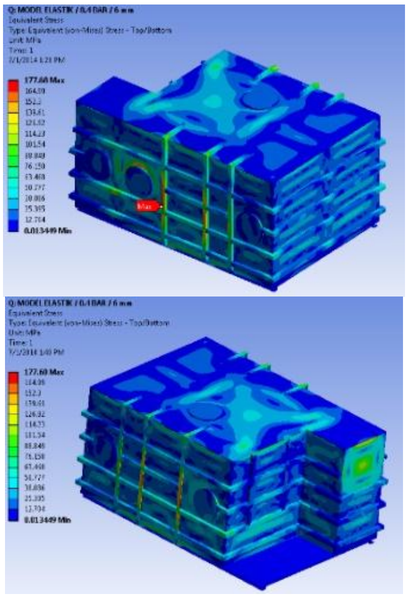

Figure 12. Von Mises stress distribution for high working loading condition (Load Case 1.2)

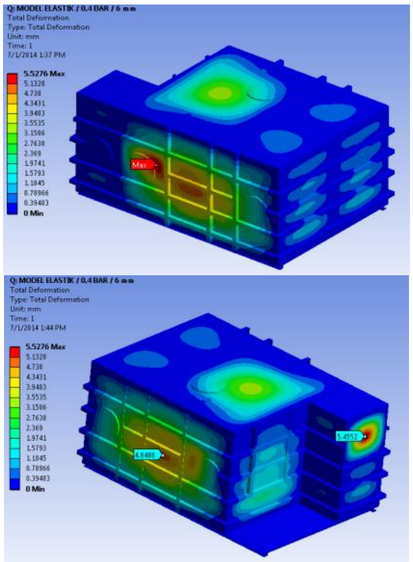

Figure 13 Deformation distribution for high working loading condition (Load Case 1.2)

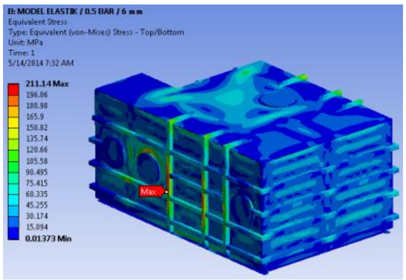

Figure 14 Von Mises stress distribution for maximum working loading condition with a linear-elastic material model (Load Case 2.1)

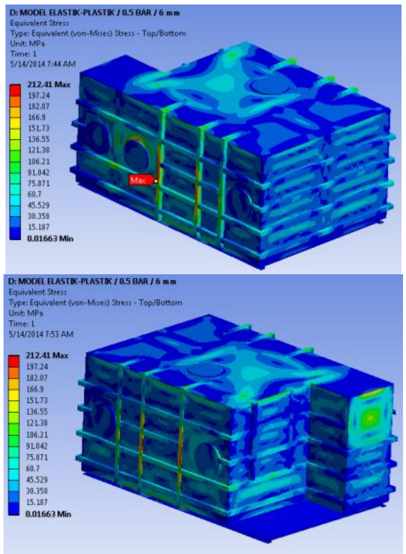

Figure 15 Von Mises stress distribution for maximum working loading condition with the elastic-plastic material model (Load Case 2.2)

The solution for deformation Figure 16 and Figure 17 for linear-elastic and elastic-plastic material model, respectively. The highest deformation value is 6.62 mm and 6.68, for linear-elastic and elastic-plastic, respectively. It occurs at the same location, i.e. around the manhole at the left side wall. Comparing the two material models results, the meshing model and the elastic-plastic material model are reliable and provide an accurate solution. Moreover, it can be concluded that under the maximum working loading caondition, there is no plastic deformation, or the tank is still safe. The current condition must have occurred under a more severe loading than the top working loading condition.

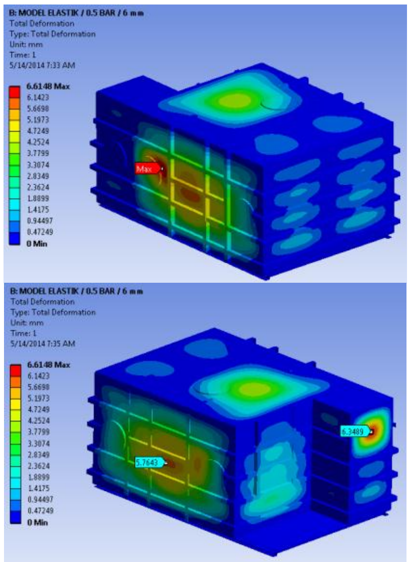

Figure 16 Deformation distribution for maximum working loading condition with a linear-elastic material model (Load Case 2.1)

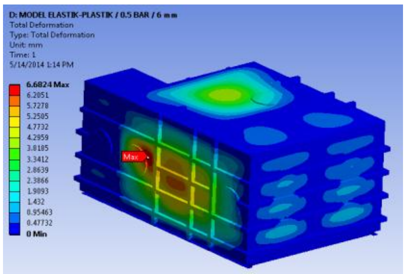

Figure 17 Deformation distribution for maximum working loading condition with an elastic-plastic material model (Load Case 2.2)

3.3 Damage Condition

Several trials of different cases have been modeled to estimate the loading condition causing the current permanent deformation as measured. The parameter to be tried includes static pressure and wall-thickness. The wall thickness measurement, it is known that the measured thickness varies between 5.35 mm and 6.08 mm, based on which the trials of thickness parameter is varied.

The static pressure is also varied for 0.5 bar (maximum allowable pressure) up to 2.5 bar, as a hypothetical value. Several combinations of the two parameters are simulated, as can be seen in Table 3.

Table 4 Load case combinations to simulate damage condition

Case No.	Static pressure (bar)	Thickness (mm)
3.01	0,5	5,80
3.02	1,0	5,35
3.03	1,5	5,67
3.04	2,0	6,00
3.05	2,1	5,35
3.06	2,2	5,35
3.07	2,3	5,67
3.08	2,4	6,00
3.09	2,5	6,00

A multi-load-step model has been used to simulate the loading-unloading condition, i.e. increasing static pressure loading up to the top value, then unloading to zero static pressure, as illustrated in Figure 18.

After several trials, it is found that three of the load cases produce a permanent deformation result close to that of measurement data. Load Case No. 3.01 (0.5 bar, 5.8 mm) is included as a benchmark, with no plastic deformation produced. Failure occurs in multiple ways for multiple reasons and does not always result in fracture [25]. Deformation theory of plasticity is applied to generalize fracture mechanics concepts to nonlinear material behavior [26]. Referring to the average thickness value, a static pressure of 2.3 bar produces a result close to the measurement data, with errors ranging from 1.35 to 7.55 % (load Case No. 3.07). The Comparison of three simulation cases with the measurement data can be seen in Table 5.

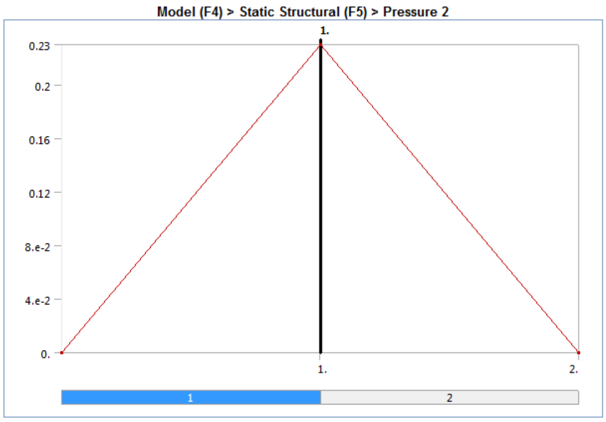

Figure 18 Multi-load-step model for modeling loading-unloading

Table 5 Comparison of three simulation cases with the measurement data. Values in square brackets represent the error in %.

	Measurement Point					
	12	13	14	15	16	17
Measurement data	**46**	**5**	**41**	**47**	**40**	**40**
Case No. 3.01 (0.5 bar, 5.8 mm, no plasticity)	1,17	0,22	1,00	1,17	0,70	1,09
Case No. 3.06 (2.2 bar, 5.35 mm)	44,77 [-2,67]	5,06 [1,20]	43,29 [5,58]	44,61 [-5,08]	36,44 [-8,90]	42,57 [6,43]
Case No. 3.07 (2.3 bar, 5.67 mm)	45,38 [-1,35]	4,91 [-1,80]	43,79 [6,80]	45,34 [-3,53]	37,54 [-6,15]	43,02 [7,55]
Case No. 3.09 (2.5 bar, 6.00 mm)	48,18 [4,74]	5,05 [1,00]	46,91 [14,41]	48,37 [2,91]	39,96 [-0,1]	46,89 [17,23]

The iteration could be resumed to obtain smaller errors, however, with several uncertainties regarding the data, the current result is considered sufficient to represent the condition of the cause of the damage and more importantly, the effect of the damage. The effect of the damage can be observed, first, in the stress distribution at the peak load, i.e. static pressure of 2.3 bar. At the peak load, the highest stress is 292.55 MPa, occurring at stiffener and several locations on the left and rightside wall Figure 19. This stress level is above the material yield strength and below its tensile strength, so that plastic deformation occurs but no breakage.

After unloading, the plastic deformation caused by pressure build-up results in residual stress, mainly on the walls (Figure 21), while Figure 22 shows the permanent deformation after unloading. The large positive Maximum Principal Stress value indicates tensile stress. In contrast, the large negative Minimum Principal Stress value indicates otherwise comparing the Maximum Principal Stress distribution during the static pressure loading process, i.e., loading at the peak load of 2.3 bar, unloading to 0 re-loading at maximum allowable working condition, 0.5 bar. It can be seen in a specific location that at the peak load, the tensile stress reaches 305 MPa, then drops to 275 MPa after unloading.

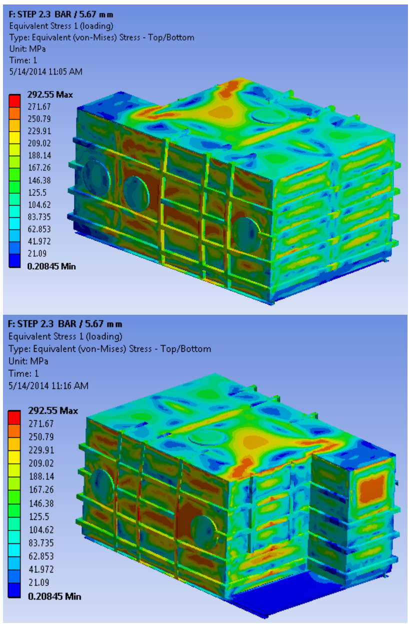

Figure 19 Von Mises stress distribution at the peak load for Load Case No. 3.07 ($_{static}$ 2.3 bar, t 5.67 mm)

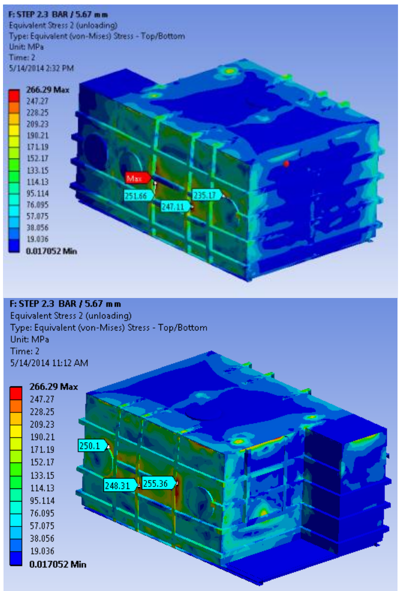

Figure 20 Von Mises stress distribution after unloading of static pressure for Load Case No. 3.07

However, according to the simulation, the stress drops to 264 MPa, when re-loaded to 0.5 bar. The stiffener's presence is considered to restrain the plate from springing back to the original condition, resulting in the plate's tensile residual stress. After re-loading, the stress is still tensile up to 0.5 bar. This condition is considered not safe. Therefore, an effort to remove the residual stress is necessary.

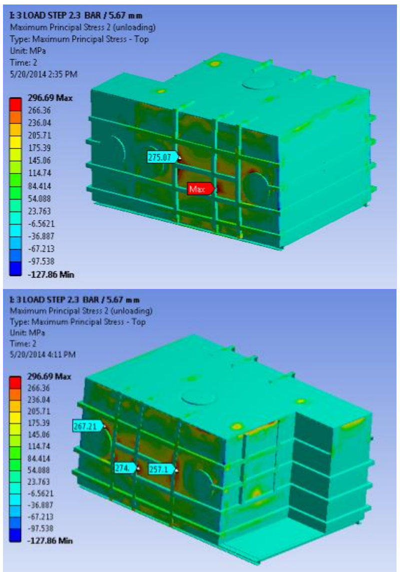

Figure 21 Maximum Principal stress distribution after unloading of static pressure for Load Case No. 3.07 (static 2.3 bar, t 5.67 mm)

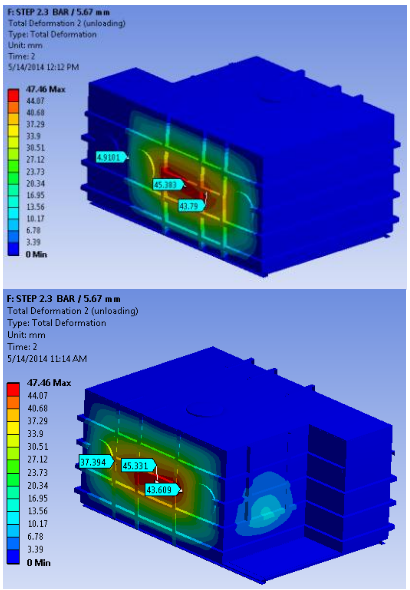

Figure 22 Permanent deformation distribution after unloading of static pressure for Load Case No. 3.07 (static 2.3 bar, t 5.67 mm)

4. CONCLUSION

A series of finite element simulations are carried out on a sewage tank model—the analysis load cases are under normal loading conditions. With a static pressure of 0.15 bar with an original thickness of 6 mm, the tank is considered safe with a safety factor is 2.87, compared with a minimum specified Yield Strength of the material of 267 MPa.

Under the highest allowable loading condition (static pressure of 0.5 bar), the safety factor drops to 1.26. After a series of simulation of damaged condition, it is concluded that the permanent deformation as inspected is estimated to be caused, by a combination of lower wall thickness than the nominal thickness, i.e., 5.67 mm (average measured thickness), and pressure accumulation of up to 2.3 bar, with errors ranging from 1.35 to 7.55 % compared to that of measurement data. With this loading case, several tank walls experience tensile residual stress. This condition is considered unsafe, primarily if the tank experience another unexpected pressure builds up. Therefore, an effort to remove the residual stress is required.

REFERENCES

1. Masuda S, Suzuki S, Sano I, Li YY, Nishimura O. The seasonal variation of emission of greenhouse gases from a full-scale sewage treatment plant. Chemosphere. 2015;
2. Anish Wankhede. Sewage Treatment Plant on Ships Explained. Marine Technology. 2019.
3. UT Report I. The measurement data of the plate thickness of Sewage Tank ST. Jakarta; 2011.
4. ASTM A36 Steel, plate. MatWEb. 2020.
5. Lubliner J, Papadopoulos P, Lubliner J, Papadopoulos P. Deformation and Strain. In: Introduction to Solid Mechanics. 2017.
6. Schajer GS. Practical Residual Stress Measurement Methods. Practical Residual Stress Measurement Methods. 2013.
7. Webster GA, Ezeilo AN. Residual stress distributions and their influence on fatigue lifetimes. Int J Fatigue. 2001;
8. Tavares SMO, de Castro PMST. Residual stress. In: SpringerBriefs in Applied Sciences and Technology. 2019.
9. Ravindranath Tagore K, Sidda Basha D. Elastic and Elasto-Plastic Finite Element Analysis of a Tension Test Specimen with and Without Voids. Int J Dev Res. 2016;
10. Dong Z, Trivedi S, Shibata Y, Tanimoto Y, Maruyama N, Nagakura M, et al. Introduction to Finite Element Analysis (FEA) or Finite Element Method (FEM). Journal of Biomechanics. 2012.
11. Patel BP, Prajapati JM. A review on FEA and optimization of backhoe attachment in hydraulic excavator. Int J Eng Technol. 2011;3(5):505.
12. Devaiah BB, Purohit R, Rana RS, Parashar V. Stress analysis of a bicycle frame. In: Materials Today: Proceedings. 2018.
13. S. A, S. A. Modeling and Analysis of the Crankshaft using ANSYS Software. In 2011.
14. AUTODESK INVESTOR. Autodesk inventor. [En línea] Available http//images.autodesk.com/adsk/files/invpro10_detail_bro__us.pdf. 2016;
15. Srinivasa-Murthy C, Wang D, Beaudoin SP, Bibby T, Holland K, Cale TS. Stress distribution in chemical mechanical polishing. Thin Solid Films. 1997;
16. Kasda K, Albayan B. Analisis Rangka Penyiang Gulma Menggunakan Metoda Elemen Hingga. MESA (Teknik Mesin, Tek Elektro, Tek Sipil, Tek Arsitektur). 2018;3(1):17–22.
17. Kim NH. Introduction to nonlinear finite element analysis. Introduction to Nonlinear Finite Element Analysis. 2015.
18. Kasda RS. Analisis Tegangan Tangki Penyimpan Berkapasitas 3000 kL dengan Cacat Geometri Ketidakbulatan. In: SNTTM XIII DEPOK. Jakarta: Universitas Indonesia; 2014.
19. Rusty Gray GT. High-strain-rate deformation: Mechanical behavior and deformation substructures induced. Annual Review of Materials Research. 2012.
20. Lee H-H. Finite element simulations with ANSYS Workbench 18. SDC publications; 2018.
21. Segalman D, Reese G, Field Jr R, Fulcher C. Estimating the probability distribution of von Mises stress for structures undergoing random excitation. J Vib Acoust. 2000;122(1):42–8.
22. Lauritano F, Runci M, Cervino G, Fiorillo L, Bramanti E, Cicciù M. Three-dimensional evaluation of different prosthesis retention systems using finite element analysis and the Von Mises stress test. Minerva Stomatol. 2016;65(6):353–67.
23. Jackson R, Chusoipin I, Green I. A finite element study of the residual stress and deformation in hemispherical contacts. J Trib. 2005;127(3):484–93.
24. Abali BE. Mechanics. In: Advanced Structured Materials. 2017.
25. Fracture Appearance and Mechanisms of Deformation and Fracture. In: Failure Analysis and Prevention. 2018.
26. Brocks W. Elastic-plastic fracture mechanics. In: Solid Mechanics and its Applications. 2018.